High-pressure band structure and structural stability of EuTe

Dhrambir Singh,[1,*] Vipul Srivastava,[1] M. Rajagopalan,[2] M. Husain,[3] and A. K. Bandyopadhyay,[1,†]
[1]*Pressure and Vacuum Standards, National Physical Laboratory, New Delhi, 110012, India*
[2]*Department of Physics, College of Engineering, Anna University, Chennai 600025, India*
[3]*Physics Department, Jamia Millia Islamia, New Delhi, India*

(Received 18 January 2000; revised manuscript received 21 June 2000; published 31 August 2001)

Band-structure calculations were carried out to study the pressure-induced structural transitions and structural stability of the magnetic compound, EuTe. The first-principle tight-binding linear muffin-tin orbital method within the local-density approximation (LDA) was used to obtain the electronic structure and total energies both at ambient as well as at high pressures. The magnetic phase stability was determined from the total-energy calculations within the atomic-sphere approximation for both nonmagnetic and magnetic phases. It is found that the magnetic phase is more stable than the nonmagnetic phase. The pure theoretical calculations further indicate that there is a phase transition from NaCl ($B1$) type to CsCl ($B2$) type structure at around 9.89 GPa, which is comparable to the experimentally observed value of 11.0 GPa. Furthermore, the bulk modulus and magnetic moments were also estimated, which were found to be in agreement with earlier experimental results.

DOI: 10.1103/PhysRevB.64.115110 PACS number(s): 71.15.Ap, 71.20.Eh, 62.50.+p

I. INTRODUCTION

The high-pressure behavior of the rare-earth (RE) monochalcognides have been investigated experimentally because of their interesting optical, magnetic, and electrical properties.[1–4] Out of these numerous RE compounds, europium monochalogenides, represented by EuX (X = O, S, Se, Te) have received a renewed attention due to their technological importance.[3–6] X-ray diffraction (XRD) and neutron-scattering studies on these EuX systems show that under normal conditions these compounds crystallize in the NaCl-type structure and the lattice parameter a decreases when X varies from Te to O.[5,6] Interestingly, these EuX compounds are semiconducting if the Eu ion is in the divalent state (2^+), while metallic if the Eu ion is in the trivalent state (3^+).[1,2] It is further reported that in some of these compounds, this valence transformation is activated under pressure,[5,6] which can be attributed to the promotion of the $4f$ electron into the $5d$ conduction-band states in the Eu ion. This pressure-induced change in valence and the subsequent semiconducting to metal transition has been ascribed as the manifestation of the valence fluctuation.[5,6] Furthermore, the pressure-volume diagram studies of EuX compounds through the systematic high-pressure XRD studies reveal that most of these compounds undergo a pressure-induced structural phase transition from $B1$ (NaCl) to $B2$ (CsCl) at a certain characteristic pressure. It is realized that both these interesting phenomena, namely, the valence fluctuations and pressure-induced structural phase transitions, can be understood only when we know precisely the ground-state properties and the nature of these electronic states in the band formation at various pressures in these systems.[6,7] The motivation of the present work is to estimate these electronic states under high pressures systematically for a system like EuTe.

It may be recalled here that EuTe, like most of the other EuX systems, undergoes a phase transformation from $B1$ to $B2$ structure at 11.0 ± 1.0 GPa at room temperature.[6] Furthermore, the qualitative optical observations up to 15 GPa showed that there was no abrupt change in the reflectivity up to 11 GPa.[6] These authors concluded that this $B1$ to $B2$ transition at 11 GPa was not accompanied by a valence change in the Eu ion, similar to the observations of EuS and also of EuSe.[6] In contrast, Rooymans[4] had earlier reported, from the high-pressure phase-equilibrium study of EuTe by XRD, that the electronic transition due to this valence change from divalent (2^+) to trivalent (3^+) state was found to occur in the pressure range 1.0–2.5 GPa. Several other studies have been reported about this material in the literature.[8–11] But to the best of our knowledge, there is no theoretical study on the structural transition and structural stability of this system under high pressures. Since we have earlier carried out band-structure calculations on the systems, such as Se,[12] Te,[13] EuSe,[14] and very recently, EuS,[15] it is tempting to take up this compound and try to complete this series purely from the theoretical point of view.

In this brief report, we present the detailed theoretical band-structure calculations of EuTe in both the phases using the tight-binding (TB) linear muffin-tin orbital (LMTO) atomic-sphere approximation (ASA) method[16–19] within the local-density approximation (LDA).[20] The compressibility behavior of this compound is discussed in light of the changes occurring in the electronic structure to study the structural stability. Both spin- and non-spin-polarized electronic band-structure calculations at ambient as well as at high pressure are performed to check nonmagnetic to magnetic or magnetic to nonmagnetic transitions in this compound. We further report the density of states (DOS), Fermi energy (E_F), lattice parameters, bulk modulus, and magnetic moment at different pressures for both the phases. The organization of the paper is as follows: Sec. II gives the method of calculations; Sec. III deals with the results and discussion in which total-energy calculations, phase transition, bulk modulus, magnetic moment, electronic structure, and phase stability are discussed; finally in Sec. IV, we have summarized the results.

II. METHOD OF CALCULATION

In our previous papers,[14,15] we have mentioned the electronic structure, total-energy, and structure stability calculations for both $B1$ and $B2$ phases by the spin-polarized TB-LMTO method. The exchange-correlation potential within the LDA was calculated using the parametrization scheme of von Barth and Hedin.[21] The DOS was calculated by the tetrahedron method.[22] Eu and Te atoms occupy the positions (0, 0, 0) and (0.5, 0.5, 0.5). The valence configurations for Eu and Te are $6s\,6p\,5d\,4f$ and $5s\,5p\,4d$, respectively. They are chosen to represent the basis set for our calculation. As already mentioned,[12–15] the TB-LMTO method works extremely well for close-packed structures; however, since EuTe in the NaCl ($B1$) phase is not a close-packed system, two equivalent empty spheres are introduced at positions (0.25, 0.25, 0.25) and (0.75, 0.75, 0.75) in such a way that they do not break the crystal symmetry.[23,24] This assumption is found to be important for total-energy calculations where the structural energy difference is only hundredths of a rydberg (Ry). Second, it is to be mentioned here that the Madelung correction, which one may neglect for the closed-packed crystal structure, is quite important for the open crystal structure. In fact, the details of the expression of the Madelung correction to the ASA have already been discussed by Skriver.[25] It is shown there that in the ASA, the Madelung expression for the electrostatic energy per ion of a lattice of point ions may be approximated by the energy of an ion embedded in a single neutralizing atom sphere. The correction term is shown to be proportional to $(1.8-\alpha_M)/S$, where α_M is the lattice Madelung constant, S is the atomic Wigner-Seitz radius, and for a closed-packed crystal structure α_M is taken as 1.8 Ry. Usually, one expresses this correction term with reference to the fcc phase, and therefore it is represented as $[(1.8-\alpha_M)_i-(1.8-\alpha_M)_{\rm fcc}]$. Skriver[25] had earlier calculated this correction term for the bcc and hcp structures relative to the fcc structure, and it is shown to be in the range 0.05–0.5 mRy when q_s/S lies in the range from 0.5 to 5 a.u.

As far as the self-consistent band calculations are concerned, they have been carried out for 512 k points for both phases in the entire Brillouin zone. To optimize these calculations, sphere radii for both cases are chosen in such a way that the difference in potentials at the sphere boundaries is minimum. Combined correction terms are also included, which account for the nonspherical shape of the atomic cells and the truncation of higher partial waves ($l>3$) inside the spheres, so that the error in the LMTO method is minimized. All relativistic corrections except those due to spin-orbit coupling are used. It is to be mentioned here that the scalar relativistic wave equation is solved in which the most important relativistic corrections, namely, Darwin's corrections, mass-velocity terms, and higher-order corrections, are included, while the spin-orbit coupling term is neglected. In other words, the radial parts of the basis function inside the muffin-tin sphere are calculated from a relativistic wave equations and the potential inside the sphere are estimated by including Darwin's corrections, mass-velocity, and higher-order correction terms. The E and K convergence are checked subsequently. The eigenvalues converge up to 10^{-5} Ry. To find the equilibrium lattice constant, the total energies are computed by changing the volume from $1.05V_0$ to $0.65V_0$, where V_0 is the equilibrium cell volume. The pressure is obtained by taking the volume derivative of the total energy and bulk modulus is calculated from the p-v diagram.

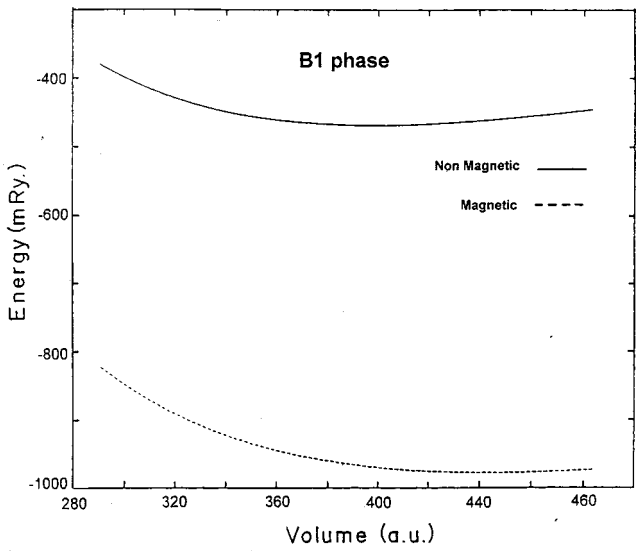

FIG. 1. Calculated total energy with cell volume for both nonmagnetic and magnetic states of the $B1$ phase.

III. RESULTS AND DISCUSSIONS

In order to obtain the ground-state properties, we have carried out self-consistent calculations for the values of total energies in magnetic and nonmagnetic states of the $B1$ phase by changing the volume as mentioned above (that is, from $1.05V_0$ to $0.65V_0$). In fact, both spin- and non-spin-polarized electronic band-structure calculations are performed for nonmagnetic and magnetic states. Figure 1 shows the variation of total energy with cell volume for both nonmagnetic and magnetic states of the $B1$ phase. It is clearly seen that there is no magnetic to nonmagnetic transition, and the magnetic state is more stable than the nonmagnetic state at ambient pressure. Similar calculations are also carried at high pressures up to 9.89 GPa; it turns out that the magnetic state is stable at all pressures in the $B1$ phase as has been shown in Fig. 1. This figure further indicates that the equilibrium cell volume in the magnetic state at ambient pressure is estimated to be 443.84 a.u.[3] Therefore, in this phase the calculated equilibrium lattice parameter a is 6.405 Å, which can be compared to the experimentally obtained value of 6.59 Å.[6] This little difference between the calculated and experimental value of a at ambient pressure will be explained in a later section.

Figure 2 shows the variation of total energy with cell volume for both the $B1$ and $B2$ phases in the magnetic state. The calculated total energies are fitted to the Birch equation of state in order to obtain the pressure-volume (p-v) relationship ($p=dE/dv$),[26] which is shown in the first inset of

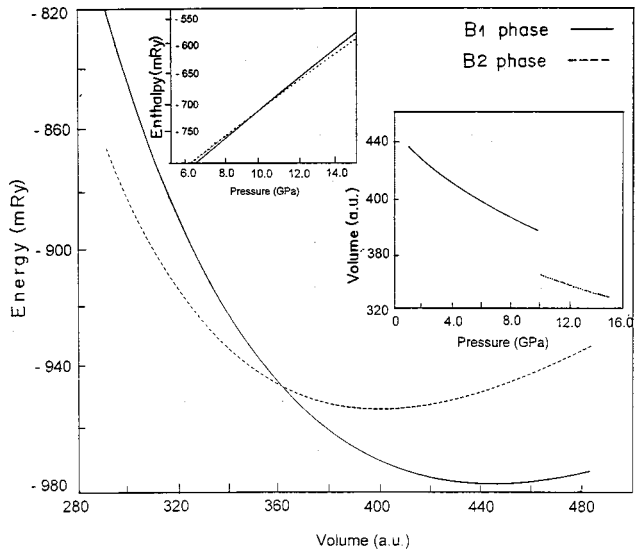

FIG. 2. The variation of total energy with cell volume for both the phases. The first inset shows the pressure-volume curve for both $B1$ and $B2$ phases. The second inset shows the variation of enthalpies with pressure in both the $B1$ and $B2$ phases.

Fig. 2 for both the phases. It can be clearly seen from these two figures that EuTe undergoes a phase transition from the $B1$ to $B2$ phase at about 9.89 GPa, which can be compared to the experimentally obtained value of 11.0 GPa. Furthermore, it may be mentioned here that in the $B1$ phase, the calculated volume reduces from 443.84 to 375.86 a.u.[3] with an increase in pressure from ambient to 9.89 GPa. The variation of lattice parameter a, at the phase transition point, due to this change in volume is estimated to be from 6.405 to 6.06 Å. This can be compared with the experimentally observed values from 6.59 to 6.22 Å.[6] Whereas in the $B2$ phase, the calculated volume just after transition is 344.92 a.u.,[3] which corresponds to an a value of 3.71 Å and this agrees comparatively well with the experimentally obtained value 3.73 Å.[6] We have further estimated the volume collapse during this phase transition, which turns out to be 8.23%, while the experimentally obtained value is 11.60%, and this small difference will be discussed later. Furthermore, the bulk modulus at zero pressure (B) is calculated using the relation $B=-V_0(dP/dV)$ from the p-v diagram and compared with available results in the literature. The theoretically calculated equilibrium bulk modulus for both $B1$ and $B2$ phases are found to be 42.1 and 101.7 GPa, respectively. On the other hand, the experimental value of the bulk modulus of the $B1$ phase is reported to be 40 ± 5 GPa,[6] but the bulk modulus for phase $B2$ has not been reported and hence comparison is not possible.

Figure 3 shows the electron dispersion curves along the high-symmetry directions in the Brillouin zone for the $B1$ (NaCl) phase just before the structural transition with a spin-down configuration. Although both spins (spin down and spin up) are estimated, only one case is depicted in Fig. 3 for reference. As mentioned, the band-structure calculation of EuTe has not been reported in literature; however, the overall profiles are found to be similar to the band structure of EuSe (Ref. 14) or EuS (Ref. 15). The Fermi energy (E_F) is shown by the dotted line. It is clear from the figure that in the valence-band region just below E_F, the lowest-lying bands arise from $5s$ states of Te, and subsequent bands are found to be predominantly due to $5p$ states of Te. However, near E_F, an Eu $4f$ state is seen. The conduction band above E_F, on the other hand, is mainly due to $5d$ and $6p$ states of Eu, and also empty states of $4f$ of Eu, etc. Figure 3 also shows the total density of states of the $B1$ phase just before structural transition, whereas the partial DOS for both spins are calculated but not shown here. As has been observed in the band structure, total DOS also shows that the lowest-energy region is mainly dominated with the $5s$ electrons of Te, and the $5p$ states are also seen in the next higher-energy region. The peak near E_F is due to $4f$ states of Eu. Similarly, the conduction band above E_F is mainly dominated by $5d$ states of Eu. Other peaks in the upper part of energy region are due to $6p$, $5d$ states and also empty states of $4f$ of Eu with $4d$ states of Te. Although partial DOS curves are not shown here, a different contribution of $4f$ electrons of Eu, $5d$ states of Eu, and $5p$ states of Te in this $B1$ phase may be clearly seen, as has been observed in the total DOS.

Figure 4 shows the electron dispersion curve along the high-symmetry directions in the Brillouin zone for the $B2$ (CsCl) phase just after transition pressure for spin-up case. Although both spins (spin down and spin up) are estimated,

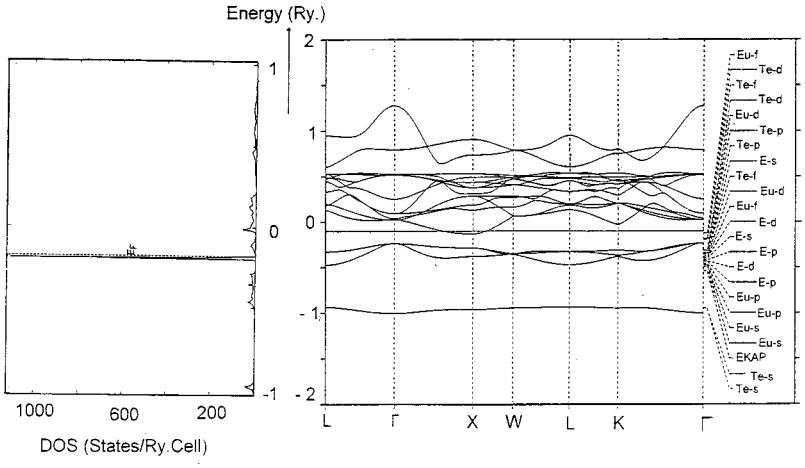

FIG. 3. Spin-down electron dispersion curves along the high-symmetry directions in the Brillouin zone with the total DOS for the $B1$ phase before the structural transition.

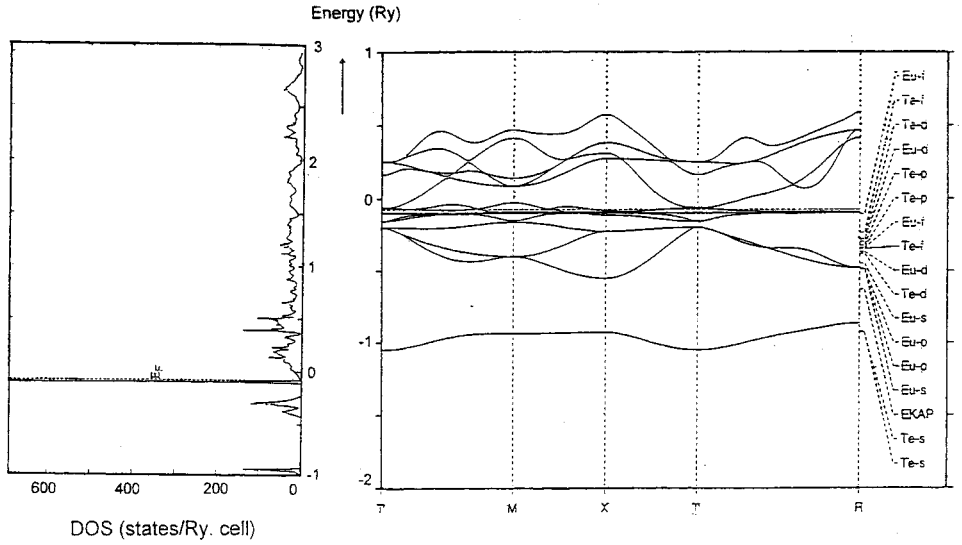

FIG. 4. Spin-down electron dispersion curves along the high-symmetry directions in the Brillouin zone with the total DOS for the $B2$ phase just after the structural transition.

for convenience, we have shown the spin-up case only. As mentioned, the lowest-lying bands arise from $5s$ states of Te, accompanied by $5p$ orbitals of Te that mainly contribute the next higher-energy states. Similarly, the total density of states of the $B2$ phase just after the structural transition is plotted in Fig. 4. It is clear that the peaks present in the lowest-energy region are mainly due to the $5s$ electrons of Te and also the $5p$ states. Here also the strong DOS peak near the Fermi energy is due to $4f$ states of Eu. The band structures and DOS for both phases are interpreted in a later section.

It may be mentioned here that the structural phase stability is determined by calculation of Gibb's free energy[27] (G) for the two phases, which is given by $G=E_{\rm tot}+PV-TS$. Since these theoretical calculations are performed at $T=0$ K, Gibb's free energy became equal to the enthalpy, $H=E_{\rm tot}+PV$. For a given pressure, a stable structure is one for which enthalpy has its lowest value. We have estimated the enthalpy for both the $B1$ and $B2$ phases and shown in the second inset of Fig. 2. It turns out that the $B1$ phase is the stable ground phase of EuTe, which is in agreement with the experimental result, and it will remain stable until the pressure reaches a value about 9.89 GPa (transition pressure). At the transition pressure, the enthalpies for the two structures are equal. But after the transition pressure, the enthalpy of the $B2$ phase becomes lower, and hence this phase becomes the stable one. The total energy versus atomic volume (Fig. 2) also confirms the phase stability of these two phases.

In order to interpret these observations, it is imperative to mention here that these total-energy calculations are based on the density-functional theory, which allows one to derive free energies, and in that way determine the atomic position in a solid such that the structure is most stable one. The chemistry of formation of the stable state of EuTe is emerging from the fact that there is charge compensation between Eu and Te atoms. In fact, Eu atom donates two electrons to the Te atom in such a way that the p bands of Te are filled. This is reflected in our band-structure calculation (indicated in Fig. 3) where the $5s$ band of Te is shown as the lowest filled band and the $5p$ bands of Te are shown as the next higher-filled bands below E_F. It is appropriate here to understand the contribution of the $4f$ state in the band formation of EuTe. The $4f$ state lies between the valence band (derived from the $5p$ states of Te) and the conduction band (derived from $5d$ states of Eu). We have calculated two cases: (1) before the phase transition ($B1$ phase) and (2) after the transition ($B2$ phase). We shall first discuss the $B1$ phase. As shown in the band structure as well as in the DOS curve (Fig. 3), this $4f$ state is represented by a sharp peak near E_F (>1100 states/Ry cell). It is quite natural that such a sharp DOS peak is an indication that the $4f$ state is a localized state. The degree of localization of this $4f$ state may be understood from the magnetic, optical, and electrical transport properties. As far as the magnetic properties are concerned, as shown in Fig. 1, one may infer that the localization of this $4f$ state is so strong that it prevents any transition from the magnetic state to the nonmagnetic state. Similarly, it is established experimentally[6] that $4f$ state heavily influences the electrical transport and optical properties of these systems under pressure. We shall now examine the case after the transition, that is, the $B2$ phase. As shown in Fig. 4 (DOS curve), this $4f$ state is represented here also by a sharp peak. However, in the $B2$ phase the number of $4f$ states reduces from 1100 to 600 states/Ry cell. This sharp decrease may be due to a fractional change in the valence state of Eu during the pressure-induced structural transition. It may be mentioned here that this fractional valence change involves a decrease in energy separation (δE_g) between the $4f$ states and the conduction-band edge with an increase in pressure. Critically the fractional delocalization of the $4f$ states is possible due to the decrease in δE_g with pressure. This is indeed observed in the experiment, where the semiconductor-metal transition has been reported under pressure.[6] Furthermore,

TABLE I. Variation of the magnetic moments (in units of μ_B) and the Madelung correction term (in Ry) as a function of V/V_0 for both phases $B1$ and $B2$.

	Magnetic moments (units of μ_B)		Madelung correction term $[(1.8-\alpha_M)_i-(1.8-\alpha_M)_{\rm fcc}]$ (Ry)	
V/V_0	$B1$ phase	$B2$ phase	$B1$ phase	$B2$ phase
1.00	6.9992	6.9999	0.013 952	−0.000 441
0.95	6.9932	6.9995	0.018 708	−0.000 401
0.90	6.9794	6.9982	0.024 682	−0.000 358
0.80	6.9331	6.9788	0.041 723	−0.000 281
0.75	6.8964	6.9575	0.053 730	−0.000 208
0.70	6.8478	6.9253	0.068 938	−0.000 152
0.65	6.7936	6.8957	0.088 631	−0.000 097

the volume change during transition in EuTe is significantly higher than that of EuS and EuSe,[6,14,15] which may also be possible due to the fractional valence change of the Eu ion during the structural transition. We may mention here that the Fermi level is shifting gradually to higher energies with an increase in pressure. This may also be explained from the fact as the fractional delocalization of the $4f$ state is taking place under pressure, there is an increase in the electron concentration. This is also reflected by the conduction bandwidth (which is the difference in energy between Fermi level and lowest eigenvalue corresponding to Γ point) also becoming broader with an increase in pressure. The magnetic moments for both the phases at different V/V_0 are indicated in Table I. It is clear that the magnetic moments decrease with an increase in pressure, which is quite natural in this kind of magnetic material.[27]

We may now concentrate our discussion on the pressure-induced structural phase transition. We might have noticed that under pressure the system proceeds from a lower coordinated NaCl (sixfold coordination) to a higher coordinated system CsCl (eightfold coordination) so as to obtain more stable state. It is also observed that the structure of any phase is determined by the competition between the energy gained by the formation of bonds and the gain in Madelung energy due to a larger coordination number (as in case of the $B2$ phase at high pressure). It is, therefore, appropriate to check the change in Madelung energy under pressure. As mentioned, in the ASA the Madelung expression is approximated by the energy of an ion embedded in a single neutralizing atomic sphere. Based on this consideration and to deal with the problem of open structure, we have introduced the Madelung correction term $[(1.8-\alpha_M)_i-(1.8-\alpha_M)_{\rm fcc}]$ in our program as discussed by Skriver.[25] The calculated correction term is shown in Table I for both the phases at all V/V_0 values. It is clear that this correction term is positive for the $B1$ phase but it is considerably low with negative sign in the $B2$ phase. The positive and negative sign is not unusual due to the fact that it is a relative term with reference to the fcc phase.[25] However, interestingly, in both phases, the correction term increases with an increase in the V/V_0 value or with pressure. It may be mentioned here that as the pressure increases, electrostatic energy increases as the atom (and therefore their nuclei) come closer. It is possible that the systematic increase of the Madelung correction term with V/V_0 or pressure may be the manifestation of this increase of electrostatic energy with pressure. As a result, the $B1$ phase is unstable at a certain pressure and undergoes a structural phase transition to the $B2$ phase above that pressure.

Finally, we shall briefly explain the disagreement of the observed values with the experimental values. For example, the calculated lattice parameter a, transition pressure, etc., are found to be slightly less than the experimental values. It is very difficult at this stage to pinpoint the exact quantitative explanation of this disagreement. However, intuitively, one may argue for several reasons, which may be categorized as follows:

(1) These theoretical calculations are done at 0 K, whereas the experimental results are obtained at room temperature.

(2) These differences may also be due to the well-known LDA contraction (i.e., the systematic overestimation of the chemical bond in a LDA treatment).

(3) These differences may be due to the uncertainties in the sphere radii chosen.

(4) These differences may be due to the introduction of the empty spheres.

As far as the thermal expansion effect is concerned, we may mention here the same analogy, $P=(G-E_{\rm tot}+TS)/V$, and since the calculations are carried out at $T=0$ K, therefore, the theoretically obtained P is always lower than that of the value obtained at room temperature. Regarding the LDA contraction, it is often found that the LDA leads to some overbinding that yields lattice parameters that are somewhat smaller when compared with experiment. However, full-potential (FP) calculations with LDA may yield a smaller equilibrium volume, which leads to better overall agreement with experiment. Regarding uncertainties in the sphere radii chosen for both cases, we have already mentioned that sphere radii are chosen in such a way that the difference in potentials at the sphere boundaries is a minimum, which may be one of the limitations. Finally, we have introduced empty spheres, which although selected in such a way that there should not be any appreciable effect on the estimation of total energy, it might still contribute, which is once again one of the limitations of this TB-LMTO method. From the above-mentioned reasons, thermal expansion and LDA contraction play a major role in the estimation. However, it would be worthwhile to extend the full-potential method studies with LDA for further improvement in the results.

IV. SUMMARY OF RESULTS AND CONCLUSIONS

The scalar-relativistic electronic band-structure calculations are obtained for both the $B1$ and $B2$ phases of EuTe using the TB LMTO method. The phase stability has been studied using the total-energy calculations for which the eigenvalues are converged up to 10^{-5} Ry. Our results show that EuTe is a stable magnetic state and there is no nonmagnetic to magnetic or magnetic to nonmagnetic transition. From the energy-volume relation we find that EuTe is stable in the $B1$ phase at ambient pressure and it undergoes a phase

transition from the $B1$ to $B2$ phases at around 9.89 GPa. The calculated lattice parameters, transition pressure, and volume collapse are compared with experimentally observed results. The bulk modulus and magnetic moments are found to be in agreement with earlier experimental results.

ACKNOWLEDGMENTS

The authors are thankful to Dr. Krishan Lal, Director, NPL, New Delhi for his continued support. Financial assistance from DST (India) is gratefully acknowledged.

*Present address: M. M. Engineering College, Mullana, Ambala (Haryana), India.

†Email: akband@csnpl.ren.nic.in

[1] F. J. Ried, L. K. Matsan, J. F. Miller, and R. C. Maines, J. Phys. Chem. Solids **25**, 969 (1964).

[2] R. Didchenko and F. P. Gortsema, J. Phys. Chem. Solids **24**, 863 (1963).

[3] Ryouichi Akimoto, Michihiro Kobayashi, and Takashi Suzuki, J. Phys. Soc. Jpn. **62**, 1490 (1993).

[4] C. J. M. Rooymans, Solid State Commun. **3**, 421 (1965).

[5] A. Chatterjee, A. K. Singh, and A. Jayaraman, Phys. Rev. B **6**, 2285 (1972).

[6] A. Jayaraman, A. K. Singh, A. Chatterjee, and S. U. Devi, Phys. Rev. B **9**, 2513 (1974).

[7] C. Basu Chaudhuri, G. Pari, A. Mookerjee, and A. K. Bhattcharjee, Phys. Rev. B **60**, 11 846 (1999).

[8] M. Umehara, J. Appl. Phys. **69**, 6028 (1991).

[9] M. Ishizuka and K. Amaya, Rev. Sci. Instrum. **66**, 3307 (1995).

[10] H. Fujiwara, H. Kadomatsu, M. Kurisu, T. Hihara, K. Kojima, and T. Kanigaichi, Solid State Commun. **42**, 509 (1982).

[11] N. Lotter and J. Wittig, J. Phys. E **22**, 440 (1989).

[12] Dharmbir Singh, A. K. Bandyopadhyay, M. Rajagopalan, P. Ch. Sahu, M. Yousuf, and K. Govinda Rajan, Solid State Commun. **109**, 339 (1999).

[13] A. K. Bandyopadhyay and Dhrambir Singh, Pramana, J. Phys. **52**, 303 (1999).

[14] Dharmbir Singh, M. Rajagopalan, and A. K. Bandyopadhyay, Solid State Commun. **112**, 39 (1999).

[15] Dharmbir Singh, M. Rajagopalan, M. Husain, and A. K. Bandyopadhyay, Solid State Commun. **115**, 323 (2000).

[16] M. Inoue, J. Phys. Soc. Jpn. **26**, 1186 (1969).

[17] O. K. Andersen, Phys. Rev. B **12**, 3060 (1975).

[18] O. K. Andersen and O. Jepsen, Phys. Rev. Lett. **53**, 2571 (1984); O. Jepsen, Phys. Rev. B **34**, 5253 (1986).

[19] D. J. Chadi, Phys. Rev. Lett. **72**, 534 (1994).

[20] W. Kohn and L. J. Sham, Phys. Rev. **140**, A1133 (1965).

[21] U. von Barth and L. Hedin, J. Phys. C **5**, 1629 (1972).

[22] O. Jepsen and O. K. Andersen, Solid State Commun. **9**, 1763 (1971).

[23] N. E. Christensen, Phys. Rev. B **32**, 207 (1985).

[24] G. Kalpana, B. Palanivel, and M. Rajagopalan, Phys. Rev. B **50**, 12 318 (1994).

[25] H. L. Skriver, Phys. Rev. B **31**, 1909 (1985).

[26] F. Birch, J. Geophys. Res. **83**, 1257 (1978).

[27] G. Kalpana, B. Palanivel, B. Kousalya, and M. Rajagopalan, Physica B **191**, 287 (1993).